Polar Geosci., **15**, 1-16, 2002

Peak temperatures of ultra-high temperature metamorphism of the Napier Complex, Enderby Land, East Antarctica, as deduced from porphyroclastic pyroxenes of meta-ultramafic rocks

Hideo Ishizuka[1], Satoko Suzuki[2] and Aki Nakamura[1]

[1]*Department of Geology, Kochi University, 2-5-1, Akebono-cho, Kochi 780-8520*
[2]*Graduate School of Science and Technology, Niigata University, Igarashi, Niigata 950-2181*

Abstract: In the Mt. Riiser-Larsen area of the Archaean Napier Complex, an ultra-high temperature (UHT) metamorphic complex, Enderby Land, East Antarctica, meta-ultramafic rocks occur as blocks and pods embedded in orthopyroxene felsic gneiss or garnet felsic gneiss and as thin layers intercalated with orthopyroxene felsic gneiss. They consist mainly of olivine, orthopyroxene, clinopyroxene and spinel with or without phlogopite. On the basis of the modal proportion of olivine and pyroxene, they are classified into peridotite and minor pyroxenite. These constituent minerals are generally medium- to coarse-grained with granular texture. Furthermore, some samples also contain coarse-grained but porphyroclastic clino- and orthopyroxenes that are sometimes armored locally by neoblastic pyroxenes. Chemical compositions of granular pyroxenes are similar to those of neoblastic varieties, which are, however, different from those of porphyroclastic pyroxenes; porphyroclastic clinopyroxenes are rich in Al_2O_3 but poor in CaO as compared with granular and neoblastic clinopyroxenes. The pyroxene thermometer yields 600–650°C for granular and neoblastic pyroxenes, while porphyroclastic pyroxenes indicate about 1130°C. The former lower temperatures are interpreted as representing a closure temperature of the thermometer, while the latter higher temperatures indicate a peak metamorphic temperature of the Napier UHT metamorphism.

key words: meta-ultramafic rocks, Mt. Riiser-Larsen, Napier Complex, peak temperatures, porphyroclastic pyroxenes

1. Introduction

Widespread occurrences of unique metamorphic minerals and mineral associations such as osumilite, inverted pigeonite, sapphirine+quartz, spinel+quartz, and sillimanite+orthopyroxene+garnet are characteristic of the Mt. Riiser-Larsen area in the Archaean Napier Complex, Enderby Land, East Antarctica (Fig. 1) (*e.g.*, Ishizuka *et al.*, 1998; Ishikawa *et al.*, 2000). Phase relations and related experiments provide unequivocal evidence that such unique minerals and mineral associations are stable under extremely high temperature conditions above 1000°C, which is generally referred to as ultra-high

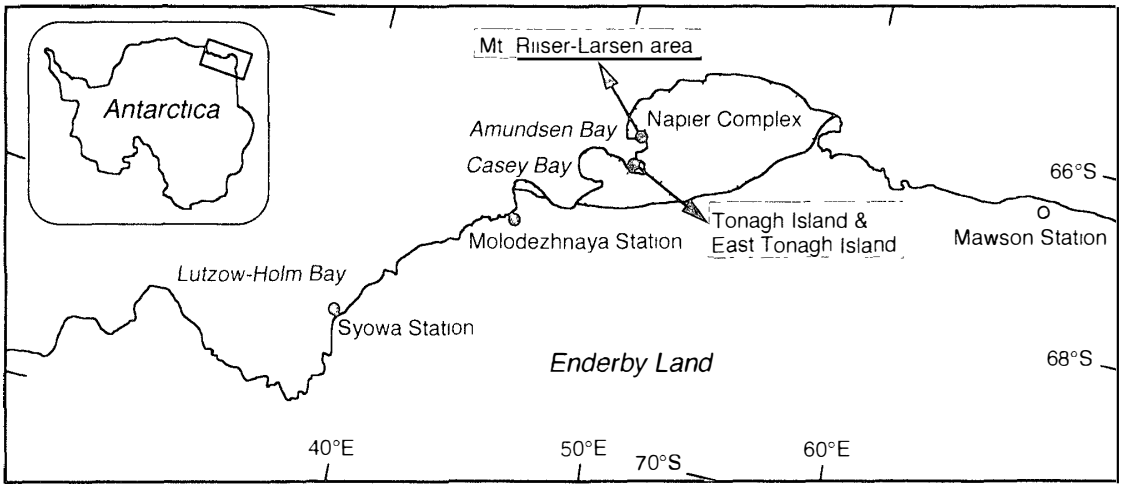

Fig. 1. Locality map of the Mt. Riiser-Larsen area, Enderby Land, East Antarctica.

temperature (UHT) metamorphism (*e.g.*, Spear, 1993; Harley, 1998). Studies on UHT metamorphism possibly lead to the recognition of several fundamental attributes such as physico-chemical conditions during stabilization of the continental crust. It is, however, very hard to estimate quantitatively the peak metamorphic conditions of UHT metamorphism, especially the peak metamorphic temperature, by the thermometric approach using chemical compositions of constituent minerals, because the low-temperature chemical re-equilibration has been generally attained during the retrograde stage that masks or obliterates the mineral compositions related to the peak metamorphic stage. Such approaches for the Napier Complex have been done only by Sandiford and Powell (1986, 1988), Harley (1987), Harley and Motoyoshi (2000) and Hokada (2001). In the course of petrographical work on meta-ultramafic rocks from the Mt. Riiser-Larsen area, we have found the pyroxenes that retain compositions equilibrated under the peak metamorphic temperatures. The following is the petrographical description of the newly found meta-ultramafic rocks along with the discussion of their significance in evaluating the thermal conditions of the Napier UHT metamorphism.

2. Field occurrence and sample description

The Mt. Riiser-Larsen area is located in the western part of the Napier Complex (Fig. 1), and is underlain by UHT metamorphic rocks and unmetamorphosed doleritic intrusive rocks The generalized geology of the area has been recently given by Ishizuka *et al.* (1998) and Ishikawa *et al.* (2000), showing that its lithology is largely divided into the layered gneiss series and massive gneiss series (Fig. 2). The layered gneiss series, occurring in the central to northwestern part of the area, is characterized by the development of various-sized layers of garnet felsic gneiss, orthopyroxene felsic gneiss, pelitic and mafic gneisses, metamorphosed impure quartzite, and metamorphosed quartz-magnetite rock. The massive gneiss series is predominant in the southern to southeastern part and consists mainly of the massive orthopyroxene felsic gneiss, in which the layering structure is not conspicuous and the lithology is rather monotonous. However, these two gneiss series are not mutually exclusive, and indeed, transitional varieties referred to as the transitional

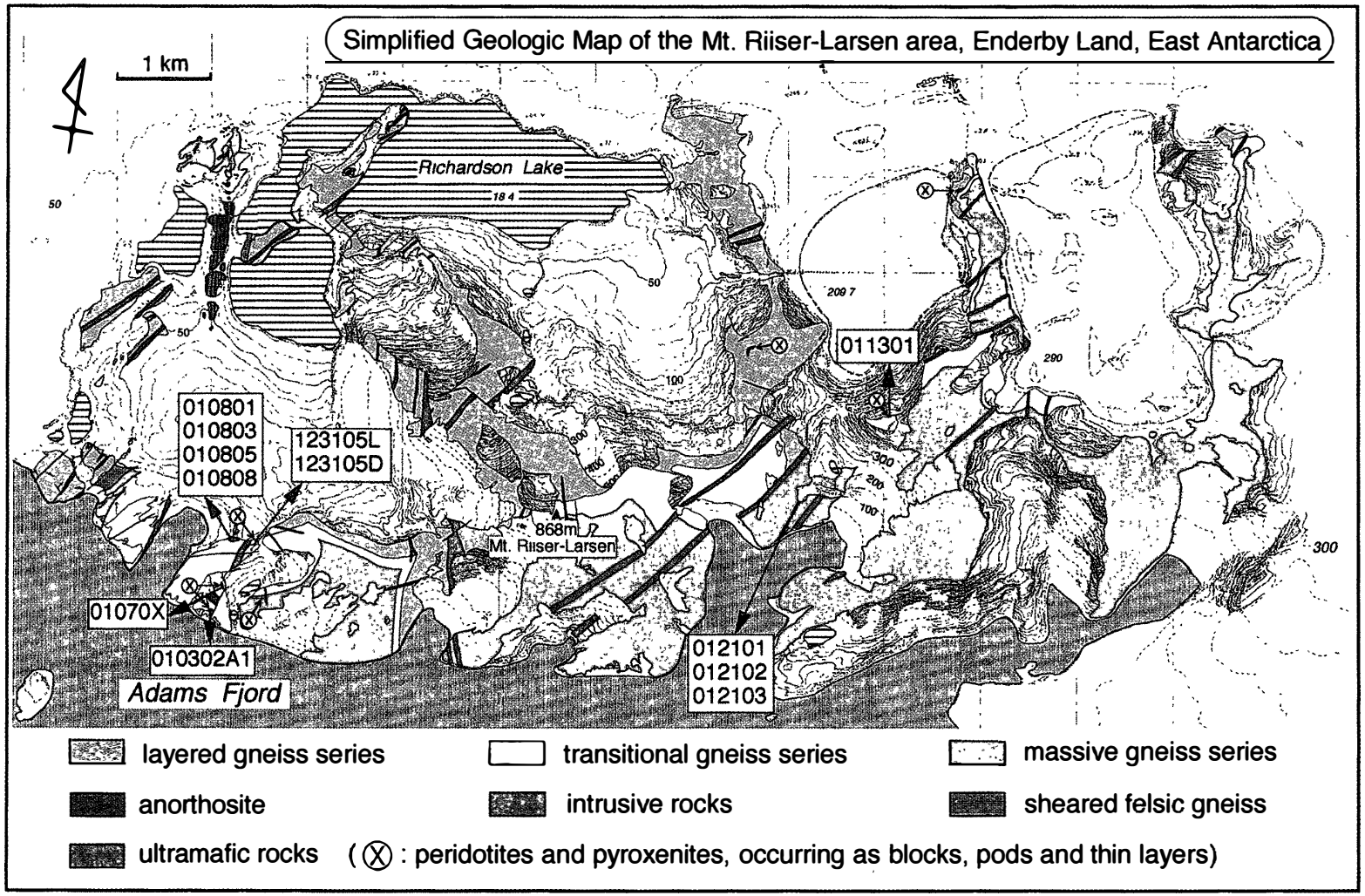

Fig. 2. Simplified geologic map of the Mt. Riiser-Larsen area (after Ishizuka et al., 1998). Sample localities of meta-ultramafic rocks analyzed here are shown along with sample numbers.

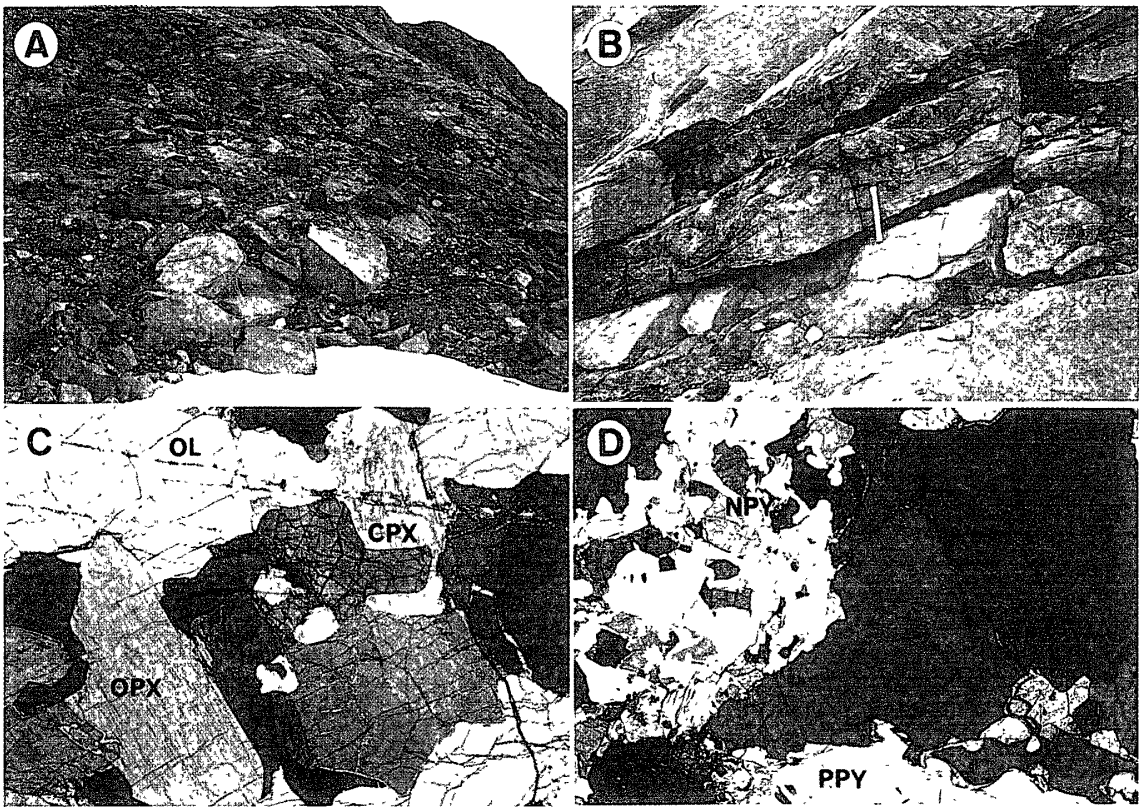

Fig. 3. Field occurrences and photomicrographs of meta-ultramafic rocks. A: Blocks of meta-ultramafic rocks (yellow-colored rocks) embedded within orthopyroxene felsic gneiss, B: Thin layer of meta-ultramafic rocks (yellow-colored rocks) interlayered with orthopyroxene felsic gneiss, C: Granular texture of meta-ultramafic rocks composed of olivine (OL), orthopyroxene (OPX) and clinopyroxene (CPX) (width = 4.0 mm), D: Porphyroclastic pyroxene (PPY) and neoblastic pyroxene (NPY) of meta-ultramafic rocks (width = 4.0 mm).

gneiss series (Ishizuka *et al.*, 1998) occur between the two gneiss series.

Meta-ultramafic rocks to be described in detail herein occur characteristically in or near the transitional gneiss series, as mappable- to unmappable-sized blocks or pods in orthopyroxene felsic gneiss or garnet felsic gneiss, and as thin layers intercalated with orthopyroxene felsic gneiss (Fig. 3A and 3B). They are commonly massive with pale yellow in color, but rarely display weak metamorphic foliation defined by elongated orthopyroxene. Petrographically, the meta-ultramafic rocks generally exhibit medium- to coarse-grained granular texture. Constituent minerals include olivine, orthopyroxene, clinopyroxene with minor amounts of spinel. Modal proportions of olivine and pyroxene classify the meta-ultramafic rocks mainly as peridotite with minor pyroxenite. Granular pyroxenes sometimes contain pronounced exsolution lamellae. Phlogopite is sometimes present but as small amounts. Of particular interest is the rare development of porphyroclastic ortho- and clinopyroxenes, which are found in only two samples, the phlogopite-free and -bearing peridotites. The porphyroclastic pyroxenes are sometimes armored locally by neoblastic ortho- and/or clinopyroxenes (Fig. 3C and 3D), in which crystal orientation as defined by cleavage is different between neoblastic and porphyroclastic pyroxenes. No replacement texture by neoblastic pyroxenes is found along or around porphyroclastic

pyroxenes. Neoblastic pyroxenes sometimes exhibit exsolution lamellae, but porphyroclastic pyroxenes show little evidence of exsolution.

3. Mineral compositions

Chemical analyses of constituent minerals by using EPMA (JEOL-8600M) at Kochi University were performed for 12 samples of meta-ultramafic rocks, 7 peridotite samples and 5 pyroxenite samples. Sample localities are shown in Fig. 2, and representative mineral analyses are listed in Tables 1 to 5. Of these samples, two peridotites, phlogopite-free (No. 7010801) and -bearing (No. 7012101) peridotites, contain porphyroclastic pyroxenes. In the Tables and the following description, FeO*means total iron as FeO, *XMg* represents the $Mg/(Mg+Fe^{2+})$ ratio of minerals, and, for spinel analyses, FeO and Fe_2O_3 were calculated from total iron assuming ideal spinel formula.

Phlogopite (Fig. 4A): The *XMg* of phlogopites from the peridotites with no porphyroclastic pyroxenes ranges from 0.93 to 0.96, and their TiO_2 contents are of 1.0 to 5.3 wt%. As compared with these phlogopite compositions, phlogopites from the peridotite (No. 7012101) with porphyroclastic pyroxenes have similar *XMg* (about 0.94) but lower TiO_2

Table 1 Representative chemical compositions of phlogopites.

	Peridotite				Pyroxenite	
	7010803	7011301	7012101	6123105D	7012102	701070X
SiO2	40.15	39.96	41.11	41.15	41.82	41.49
TiO2	3.27	3.40	0.95	2.81	2.48	1.53
Al2O3	13.75	15.70	16.28	13.68	13.43	15.03
Cr2O3	0.25	1.27	0.64	0.35	0.11	0.47
FeO*	2.10	3.04	3.02	1.94	2.69	3.04
MnO	0.02	0.01	0.06	0.00	0.07	0.01
MgO	25.84	24.51	26.15	25.66	26.54	25.32
NiO	0.09	0.15	0.21	0.12	0.23	0.42
CaO	0.05	0.02	0.01	0.01	0.00	0.03
Na2O	0.40	0.14	0.09	0.51	0.28	0.16
K2O	10.31	8.68	7.96	10.08	9.54	8.84
P2O5	0.10	0.05	0.00	0.01	0.02	0.06
Total	96.30	96.90	96.47	96.33	97.20	96.42
O=22.0						
Si	5.612	5.519	5.650	5.727	5.761	5.740
Ti	0.343	0.353	0.098	0.294	0.257	0.160
Al	2.266	2.556	2.637	2.245	2.182	2.452
Cr	0.028	0.139	0.069	0.039	0.012	0 052
Fe*	0.246	0.351	0.347	0.225	0.310	0.352
Mn	0.003	0.001	0.007	0.000	0.008	0.002
Mg	5.383	5.045	5.355	5.323	5.450	5.221
Ni	0.010	0.016	0.023	0.014	0.025	0.047
Ca	0.007	0.003	0.001	0.002	0.000	0.005
Na	0.107	0.037	0.023	0.138	0.076	0.043
K	1.838	1.529	1.396	1.790	1.676	1.561
P	0.011	0.006	0.000	0.001	0.002	0 007
Total	15.853	15.555	15.608	15.799	15.758	15.640
XMg	*0.96*	*0.94*	*0.94*	*0.96*	*0.95*	*0.94*

Table 2. Representative chemical compositions of spinels.

	Phl-free Peridotite			Phl-bearing Peridotite				Phl-bearing Pyroxenite		Phl-free Pyroxenite
	7010801	6123105L	7010805	7010803	7011301	7012101	6123105D	701070X	7012102	7012103
SiO_2	0 03	0.00	0.00	0 04	0.02	0.00	0.05	0.03	0.06	0.04
TiO_2	0 01	0.06	0.03	0.05	0.04	0.00	0 00	0 00	0.02	0.02
Al_2O_3	61 91	58.84	58.58	56.22	38.97	57.61	62.71	48 25	59 71	59.76
Fe_2O_3	1 73	0.67	0.69	2.67	1.70	3.12	0 68	2.52	4 13	2.37
Cr_2O_3	5 84	11.83	10.24	10 28	29.70	8.89	7 30	18 59	4.96	6 22
FeO	7 75	8 72	9 90	11.77	16 35	11.55	7 84	15 25	13 22	15 31
MnO	0.05	0 17	0.09	0.04	0.23	0.06	0 12	0.17	0.15	0.11
MgO	21.94	21 35	20.25	18.82	14 36	19.15	21 96	15 49	18 08	16 73
NiO	0.38	0.08	0 42	0 41	0.14	0.33	0 52	0.51	0.69	0.58
CaO	0.00	0 00	0.02	0.01	0.00	0.03	0.00	0 02	0.02	0 04
Na_2O	0.00	0 03	0.00	0 02	0.02	0.02	0 08	0.08	0.03	0 07
K_2O	0 00	0.00	0.00	0.00	0.00	0.00	0.00	0.00	0.00	0 00
P_2O_5	0 00	0.00	0.01	0 01	0.00	0.02	0 03	0.03	0.02	0 00
Total	99 63	101.74	100.23	100.33	101.53	100.77	101 29	100 92	101.08	101 24
O=4.0										
Si	0.001	0 000	0.000	0.001	0 001	0.000	0.001	0.001	0 001	0 001
Ti	0.000	0.001	0.001	0.001	0.001	0 000	0 000	0.000	0.000	0 000
Al	1.848	1.753	1 777	1.732	1.298	1.758	1 844	1.550	1 816	1.827
Fe^{3+}	0 033	0.013	0.013	0 053	0.036	0.061	0.013	0.052	0.080	0.046
Cr	0 117	0.236	0.208	0.212	0.664	0.182	0 144	0.400	0.101	0.128
Fe^{2}	0 164	0 184	0.213	0 257	0.386	0.250	0.164	0.348	0.285	0.332
Mn	0.001	0.004	0.002	0 001	0.005	0.001	0 003	0.004	0 003	0.002
Mg	0 828	0.804	0 776	0 733	0 605	0 739	0.816	0 629	0.695	0.647
Ni	0 008	0.002	0 009	0.009	0 003	0 007	0 010	0 011	0 014	0.012
Ca	0 000	0.000	0.001	0.000	0 000	0.001	0.000	0.000	0.000	0.001
Na	0.000	0.001	0.000	0.001	0.001	0.001	0.004	0.004	0.002	0.004
K	0.000	0 000	0.000	0.000	0.000	0.000	0 000	0.000	0.000	0 000
P	0.000	0 000	0.000	0 000	0 000	0 001	0.001	0 001	0.000	0 000
Total	3.000	2 998	3.000	3 000	3 000	3 000	3 000	2.999	3.000	3.000
XMg	*0.83*	*0.81*	*0.78*	*0 74*	*0.61*	*0.75*	*0.83*	*0 64*	*0.71*	*0 66*

Table 3. Representative chemical compositions of olivines.

	Phl-free Peridotite			Phl-bearing Pridotite				Phl-bearing Pyroxenite
	7010801	7010805	6123105L	7010803	7011301	7012101	6123105D	7012102
SiO_2	42 63	40.45	40.53	40.23	40.35	38.14	41.49	38.14
TiO_2	0.00	0.01	0.00	0.00	0.02	0.02	0.03	0.02
Al_2O_3	0.00	0.00	0.00	0.06	0.00	0.03	0.01	0 03
Cr_2O_3	0.00	0.04	0.00	0.00	0.06	0.03	0.01	0.03
FeO*	5 93	7.08	7.09	9.76	7.48	10.65	6.42	10.65
MnO	0.16	0.07	0.14	0.10	0.11	0.16	0.14	0.16
MgO	50 95	52.34	52.01	49.72	52.63	51.34	52.34	51.34
NiO	0.47	0.40	0.48	0.53	0.43	0.51	0.50	0.51
CaO	0.00	0.01	0.00	0.00	0.05	0.02	0.00	0.02
Na_2O	0.02	0.01	0.00	0.00	0.00	0.04	0.00	0.04
K_2O	0.00	0.00	0.00	0.00	0.00	0.00	0.00	0 00
P_2O_5	0.00	0 04	0.00	0.00	0.03	0.00	0.03	0.00
Total	100.17	100.44	100.25	100.39	101 16	100.92	100.96	100.92
O=4.0								
Si	1.023	0.978	0.983	0.985	0.972	0.939	0.994	0 939
Ti	0.000	0.000	0.000	0.000	0.000	0.000	0.001	0.000
Al	0.000	0.000	0.000	0.002	0.000	0.001	0.000	0.001
Cr	0 000	0.001	0.000	0.000	0.001	0.001	0.000	0.001
Fe*	0.119	0 143	0.144	0.200	0.151	0.219	0.129	0.219
Mn	0.003	0.001	0.003	0.002	0 002	0.003	0.003	0.003
Mg	1.822	1.887	1.879	1 815	1.889	1.885	1.868	1.885
Ni	0.009	0.008	0.009	0.010	0.008	0.010	0.010	0.010
Ca	0.000	0.000	0.000	0.000	0.001	0.000	0.000	0.000
Na	0.001	0.000	0.000	0.000	0.000	0.002	0.000	0.002
K	0.000	0.000	0.000	0.000	0.000	0.000	0.000	0.000
P	0.000	0.001	0.000	0.000	0.001	0.000	0.001	0.000
Total	2.977	3.020	3.017	3 014	3.026	3.060	3.005	3.060
XMg	*0.94*	*0.93*	*0.93*	*0.90*	*0.93*	*0.90*	*0.94*	*0.90*

Table 4. Representative chemical compositions of granular pyroxenes.

	Phl-free Peridotite						Phl-bearing Peridotite					
	7010801		7010805		6123105L		7010803		7011301	7012101		6123105D
	Cpx	Opx	Cpx	Opx	Cpx	Opx	Cpx	Opx	Cpx	Cpx	Opx	Opx
SiO_2	53.28	55.67	53.60	57.87	51.51	55.78	52.83	55.06	53.02	52.38	54.87	56.55
TiO_2	0.54	0.09	0.55	0.08	1.50	0.19	0.42	0.10	0.64	0.07	0.03	0.08
Al_2O_3	4.82	3.13	4.69	2.59	3.24	3.30	3.10	3.59	2.36	3.72	2.06	1.82
Cr_2O_3	0.52	0.17	0.69	0.21	0.68	0.37	0.41	0.46	0.65	0.48	0.24	0.05
FeO*	1.50	4.37	1.58	5.59	4.87	5.00	2.91	5.54	2.56	3.32	7.56	5.41
MnO	0.00	0.13	0.09	0.19	0.33	0.11	0.08	0.15	0.08	0.07	0.23	0.15
MgO	15.63	36.64	15.24	36.04	15.53	34.79	15.67	34.59	16.66	17.49	34.91	35.28
NiO	0.07	0.05	0.04	0.08	0.01	0.08	0.03	0.19	0.01	0.00	0.05	0.09
CaO	21.73	0.38	23.08	0.16	21.59	0.44	23.01	0.59	23.15	22.23	0.33	0.12
Na_2O	1.68	0.00	0.65	0.00	0.91	0.04	0.84	0.06	1.11	0.67	0.04	0.00
K_2O	0.00	0.00	0.01	0.00	0.01	0.00	0.00	0.00	0.00	0.00	0.00	0.00
P_2O_5	0.00	0.03	0.06	0.00	0.08	0.19	0.00	0.02	0.00	0.03	0.00	0.03
Total	99.77	100.65	100.27	100.22	100.25	100.30	99.31	100.35	100.25	100.49	100.31	99.57
O=6.0												
Si	1.926	1.897	1.928	1.935	1.890	1.910	1.937	1.895	1.929	1.899	1.906	1.950
Ti	0.015	0.002	0.015	0.002	0.041	0.005	0.012	0.003	0.018	0.002	0.001	0.002
Al	0.206	0.126	0.199	0.102	0.140	0.133	0.134	0.146	0.101	0.159	0.084	0.074
Cr	0.015	0.004	0.020	0.006	0.020	0.010	0.012	0.013	0.019	0.014	0.007	0.001
Fe*	0.045	0.125	0.048	0.156	0.150	0.143	0.089	0.159	0.078	0.101	0.220	0.156
Mn	0.000	0.004	0.003	0.005	0.010	0.003	0.003	0.004	0.003	0.002	0.007	0.004
Mg	0.842	1.861	0.817	1.796	0.849	1.775	0.857	1.774	0.904	0.945	1.808	1.813
Ni	0.002	0.001	0.001	0.002	0.000	0.002	0.001	0.005	0.000	0.000	0.001	0.002
Ca	0.841	0.014	0.890	0.006	0.849	0.016	0.904	0.022	0.903	0.864	0.012	0.005
Na	0.118	0.000	0.045	0.000	0.065	0.003	0.060	0.004	0.078	0.047	0.002	0.000
K	0.000	0.000	0.000	0.000	0.000	0.000	0.000	0.000	0.000	0.000	0.000	0.000
P	0.000	0.001	0.002	0.000	0.003	0.005	0.000	0.001	0.000	0.001	0.000	0.001
Total	4.009	4.034	3.967	4.010	4.017	4.007	4.008	4.025	4.032	4.034	4.048	4.009
XMg	*0.95*	*0.94*	*0.94*	*0.92*	*0.85*	*0.93*	*0.91*	*0.92*	*0.92*	*0.90*	*0.89*	*0.92*

Table 4. Continued.

	Phl-free Pyroxenite						Phl-bearing Pyroxenite			
	7012102		7010302A1		701070X		7010808		7012103	
	Cpx	Opx	Cpx	Opx	Cpx	Opx	Cpx	Opx	Cpx	Opx
SiO_2	50.71	53.38	53.18	55.92	52.46	55.00	52.29	55.23	49.29	55.40
TiO_2	0.46	0 09	0.12	0.00	0.09	0.00	0.61	0.06	0.82	0 15
Al_2O_3	5.07	3.58	2.13	1.32	3.59	2.52	2.43	2.22	6.83	2.01
Cr_2O_3	0.21	0.20	1.48	0.35	0.55	0.35	0 34	0.23	0.29	0.20
FeO*	3.46	8.93	2.77	9.61	2.45	8.34	4.56	11.60	4.07	9.87
MnO	0.10	0.12	0.15	0.15	0.03	0.29	0.09	0.16	0 12	0.09
MgO	15.73	33.33	17.13	33.17	16.96	33.79	16.01	30.64	14.69	32 17
NiO	0.08	0.09	0.09	0.11	0.05	0.17	0.03	0.07	0 10	0.08
CaO	24.31	0.42	22.17	0.24	23 94	0 29	23.86	0.20	23.45	0.21
Na_2O	0 38	0.00	0.81	0.07	0.39	0.01	0.58	0.00	0.41	0.04
K_2O	0.00	0.00	0.00	0.00	0.00	0.00	0.00	0.00	0.00	0 00
P_2O_5	0.00	0.00	0.04	0.04	0.05	0.00	0.00	0.04	0 03	0.06
Total	100 50	100.15	100.07	100.97	100.56	100.75	100.80	100.45	100.09	100.28
O=6.0										
Si	1.853	1.870	1.937	1.943	1.901	1.909	1.912	1.942	1.811	1 880
Ti	0.013	0.002	0.003	0.000	0.003	0.000	0 017	0.001	0.023	0.004
Al	0.218	0.148	0.091	0.054	0.153	0.103	0.105	0.092	0.296	0.200
Cr	0 006	0.005	0.043	0.010	0.016	0.010	0 010	0.006	0.008	0.005
Fe*	0.106	0.262	0.085	0.279	0.074	0.242	0 139	0.341	0.125	0.280
Mn	0 003	0.003	0.005	0 004	0.001	0.008	0.003	0 005	0.004	0.003
Mg	0.856	1 741	0.930	1.718	0.916	1.748	0.872	1.606	0.805	1.627
Ni	0.002	0.003	0.002	0.003	0.002	0.005	0.001	0.002	0.003	0 002
Ca	0.952	0.016	0.865	0.009	0.930	0.011	0.935	0.007	0.923	0.008
Na	0.027	0 000	0.057	0.005	0.027	0.001	0.041	0.000	0.029	0.002
K	0 000	0.000	0.000	0.000	0.000	0.000	0.000	0.000	0.000	0.000
P	0 000	0.000	0.001	0.001	0.002	0.000	0.000	0.001	0.001	0 002
Total	4.036	4.051	4 019	4.026	4.023	4.035	4.035	4.005	4.028	4.012
XMg	*0.89*	*0 87*	*0.92*	*0.86*	*0.93*	*0.88*	*0.86*	*0.82*	*0 87*	*0.85*

Table 5. Representative chemical compositions of porphyroclastic and neoblastic pyroxenes.

	Phl-free Peridotite (7010801)				Phl-bearing Peridotite (7012101)			
	Porphyroclast		Neoblast		Porphyroclast		Neoblast	
	Cpx	Opx	Cpx	Opx	Cpx	Opx	Cpx	Opx
SiO_2	50.24	52 41	53.29	56 35	51.33	52 12	53 28	54 94
TiO_2	0.38	0.07	0.47	0.10	0.04	0.02	0.04	0 00
Al_2O_3	6.89	5 11	3 45	2.10	4 98	4 14	2.87	2.48
Cr_2O_3	0.44	0.14	0.51	0 23	0 41	0.37	0 41	0 37
FeO*	2 58	4.89	1 80	4.22	3.48	6.47	2.82	6.94
MnO	0 06	0.05	0.07	0.07	0.12	0.18	0.12	0 21
MgO	19.65	35.78	15 54	36.99	19.75	35 21	16 76	35 04
NiO	0.08	0.03	0.06	0.05	0 02	0 07	0.02	0.07
CaO	18 78	2.22	22.31	0 29	19.52	1.55	23.73	0.49
Na_2O	1.71	0.02	1.63	0.03	0.62	0.02	0.62	0.04
K_2O	0 00	0.00	0.00	0 00	0.00	0 00	0 00	0.00
P_2O_5	0.00	0 00	0 04	0.00	0.00	0 00	0.00	0 00
Total	100.81	100 72	99 17	100 42	100 27	100 15	100.66	100 56
O=6 0								
Si	1.804	1.807	1 946	1 922	1.855	1.820	1 930	1.900
Ti	0.010	0.002	0 013	0 003	0.001	0.001	0 001	0 000
Al	0.292	0 208	0 149	0.084	0.212	0.170	0 122	0 101
Cr	0.012	0.004	0 015	0.006	0.012	0.010	0 012	0 010
Fe*	0 077	0 141	0.055	0.120	0.105	0 189	0 086	0 201
Mn	0 002	0 001	0.002	0.002	0.004	0 005	0 004	0 006
Mg	1 052	1.839	0.846	1.880	1 064	1 833	0 905	1 806
Ni	0 002	0.001	0 002	0.001	0 001	0.002	0 001	0 002
Ca	0 723	0 082	0.873	0.011	0 756	0.058	0.921	0 018
Na	0.119	0.001	0 116	0 002	0 044	0.001	0 044	0.002
K	0 000	0 000	0.000	0.000	0.000	0.000	0 000	0.000
P	0 000	0.000	0.001	0.000	0.000	0.000	0.000	0.000
Total	4 093	4 086	4.016	4.031	4 053	4 090	4.024	4.046
XMg	*0 93*	*0.93*	*0 94*	*0 94*	*0 91*	*0.91*	*0 91*	*0 91*

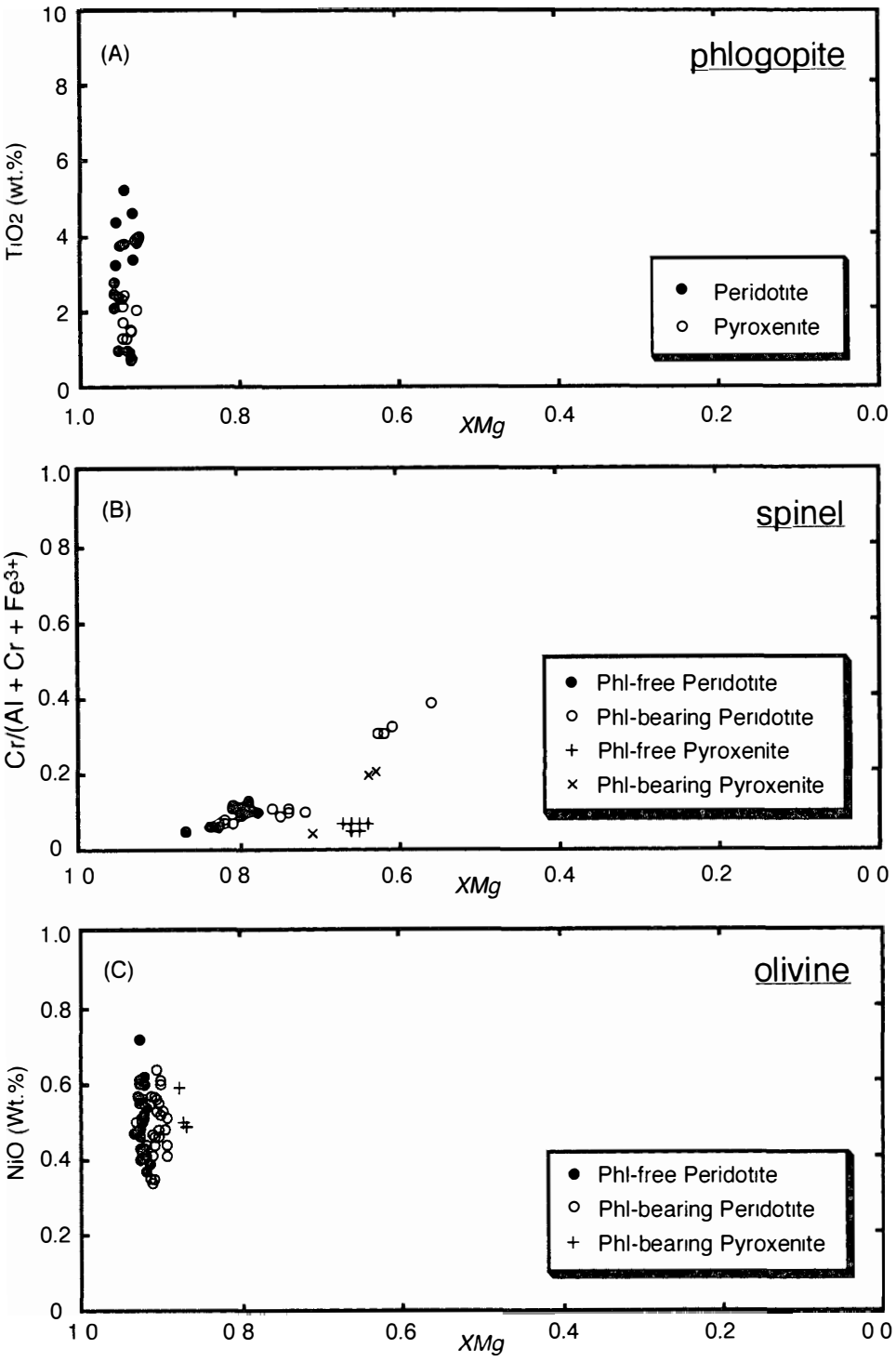

Fig. 4. Compositions of phlogopite (A), spinel (B) and olivine (C) from meta-ultramafic rocks.

contents (0.8–1.0 wt%). The phlogopite-bearing pyroxenites have phlogopites with *XMg* of 0.93 to 0.95 and TiO_2 contents of 1.3 to 2.5.

Spinel (Fig. 4B): The *XMg* and $Cr/(Cr+Al+Fe^{3+})$ ratios of spinels range in peridotites from 0.71 to 0.90 and from 0.05 to 0.12, respectively, while spinels from pyroxenites have *XMg* of 0.61 to 0.71 and a $Cr/(Cr+Al+Fe^{3+})$ ratio of 0.05 to 0.21. A

high $Cr/(Cr+Al+Fe^{3+})$ ratio (0.3–0.4) is also found in one peridotite sample with low XMg of 0.54 to 0.61.

Olivine (Fig. 4C): There is no sign of compositional heterogeneity in olivines of the analyzed samples. In the samples with no porphyroclastic pyroxenes, there is no distinct

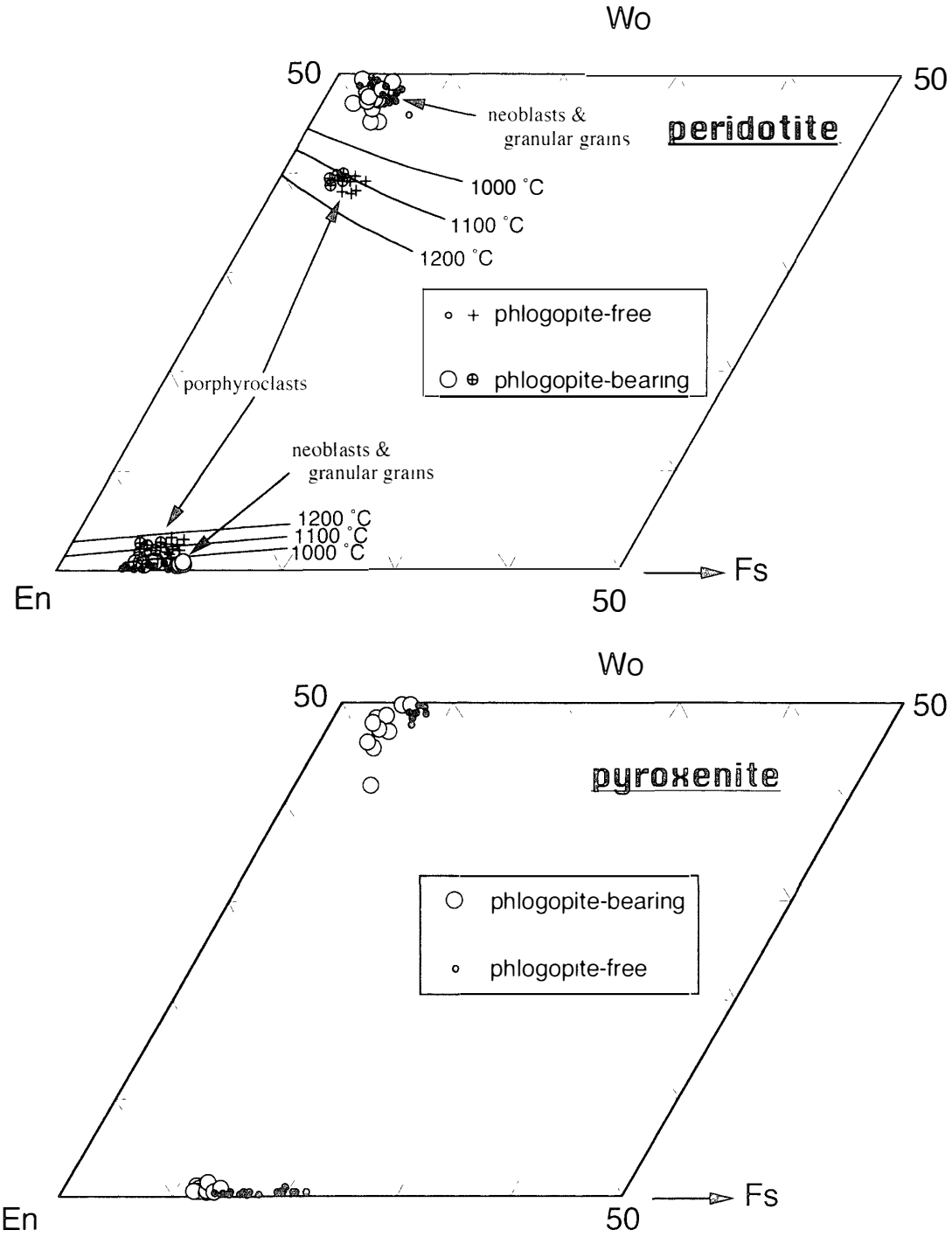

Fig. 5. Pyroxene compositions of meta-ultramafic rocks plotted in the pyroxene quadrilateral. Pyroxene thermometer at 10 kbar as shown in the upper quadrilateral is constructed after Lindsley (1983). Each component is calculated by the method of Lindsley (1983).

difference in olivine composition (XMg=0.91–0.94, NiO=0.34–0.72 wt%) between the phlogopite-free and -bearing peridotites, while olivines from the pyroxenites have XMg of 0.87 to 0.90 and NiO of 0.16 to 0.59 wt%. As compared with these data, the sample No. 7010801 (phlogopite-free) has olivines with the similar XMg (0.93–0.94) and NiO content (0.42–0.60 wt%), while olivines from the sample No. 7012101 (phlogopite-bearing) have the slightly lower XMg (about 0.90) but similar NiO content (0.41–0.52 wt%).

Orthopyroxene (Fig. 5): No chemical heterogeneity is detected within individual grains in analyzed orthopyroxenes. There is no distinct difference in composition among granular orthopyroxenes in peridotites without porphyroclastic pyroxenes; XMg=0.89–0.94, CaO=0.1–0.7 wt%, and Al_2O_3=0.8–4.9 wt%. As compared with these orthopyroxene compositions, granular and neoblastic orthopyroxenes of the phlogopite-free peridotite with porphyroclastic texture (No. 7010801) have similar XMg (0.92–0.94), and CaO (0.2–0.6 wt%) and Al_2O_3 (0.8–4.1 wt%) contents, while those of the phlogopite-bearing peridotite with porphyroclastic texture (No. 7012101) are slightly low in XMg (0.89–0.90) but similar in CaO (0.3–0.5 wt%) and Al_2O_3 (2.9–4.0 wt%). Orthpyroxenes forming exsolution lamellae in granular and neoblastic clinopyroxenes are similar in composition to those of exsolution-free granular and neoblastic orthopyroxenes, respectively. Porphyroclastic orthopyroxenes have similar XMg to granular and neoblastic varieties in the same samples, but their CaO and Al_2O_3 contents are apparently enriched; *i.e.*, CaO=1.7–2.5 wt% and Al_2O_3=4.8–5.2 wt% in No. 7010801, and CaO=1.3–1.8 wt% and Al_2O_3=4.1–4.8 wt% in No. 7012101. Orthopyroxenes in pyroxenites are lower in XMg (0.78–0.88) than those in peridotites, and their CaO and Al_2O_3 contents range from 0.1 to 0.6 and from 1.0 to 5.7 wt%, respectively.

Clinopyroxene (Fig. 5): Clinopyroxenes analyzed here are also commonly homogeneous in composition within individual grains. No compositional difference is found among granular clinopyroxenes in peridotites with no porphyroclastic texture; XMg=0.90–0.95, CaO=21.1–23.4 wt%, and Al_2O_3=2.1–4.8 wt%. As compared with these clinopyroxene compositions, granular and neoblastic clinopyroxenes of the phlogopite-free peridotite with porphyroclastic texture (No. 7010801) have similar XMg (0.94–0.95), and CaO (21.7–22.3 wt%) and Al_2O_3 (2.8.–3.5 wt%) contents, while those of the phlogopite-bearing peridotite with porphyroclastic texture (No. 7012101) are slightly low in XMg (0.89–0.92) but similar in CaO (22.2–24.4 wt%) and Al_2O_3 (2.6–3.7 wt%). Exsolution clinopyroxenes in granular and neoblastic orthopyroxenes have similar compositions to those of exsolution-free granular and neoblastic clinopyroxenes. Porphyroclastic clinopyroxenes are similar in XMg to granular and neoblastic varieties in the same samples, but their CaO content is apparently depleted and their Al_2O_3 content is enriched; *i.e.*, CaO=18.5–18.9 wt% and Al_2O_3=5.8–6.9 wt% in No. 7010801, and CaO=18.8–19.6 wt% and Al_2O_3=4.8–6.2 wt% in No. 7012101. Clinopyroxenes in pyroxenites are lower in XMg (0.84–0.93) than those in peridotites, and their CaO and Al_2O_3 contents range from 20.3 to 24.3 wt% and 1.9 to 6.8 wt%, respectively.

4. Pyroxene thermometry

As described previously, the chemical compositions of granular and neoblastic pyroxenes are similar to each other, but they are apparently different from porphyroclastic

varieties. This means that the thermal history or finally equilibrated conditions of granular and neoblastic pyroxenes are different from the conditions of porphyroclastic varieties. Compositions of other minerals in peridotites are similar to each other, and those in pyroxenites are also similar to each other; the difference in mineral compositions between peridotites and pyroxenites may be attributed to the difference in bulk rock compositions.

Conventional multi-component two-pyroxene thermometers (Wood and Banno, 1973; Wells, 1977) based on combinations of simple system experiments and empirical Fe-corrections have been superseded by projection-based quadrilateral pyroxene thermometry (Lindsley, 1983), which is used here as shown in Fig. 5. At the relevant pressures of 10 kbar (*e.g.*, Harley and Motoyoshi, 2000), the estimated temperatures make two clusters; high temperatures (up to 1130°C) as recorded by porphyroclastic pyroxenes and low temperatures (650–700°C) as indicated by granular as well as neoblastic pyroxenes are apparent from Fig. 5.

5. Discussion and conclusion

Although the geochemical study suggested that the precursors of phlogopite-free and phlogopite-bearing meta-peridotites are depleted mantle peridotites and related komatiitic rocks, respectively (Suzuki *et al.*, 1999), the original textures such as spinifex texture of these rocks were perfectly modified by metamorphism, and then, most of these rocks now display granular textures. It is, therefore, likely that granular minerals have been once equilibrated under the peak metamorphic temperature of UHT metamorphism, and subsequently they were chemically re-equilibrated during the retrograde stage to lower temperature compositions. The occurrence of porphyroclastic minerals with high temperature (up to 1130°C) compositions, as described previously, suggests that the retrograde redistribution of elements occurred perfectly in most of the rocks, but rarely it was local and produced a porphyroclastic texture that resulted in the retention of high-temperature compositions. The formation of porphyroclastic minerals helps to keep the high temperature compositions, and the high temperatures estimated from the compositions of porphyroclastic pyroxenes are interpreted as a temperature avoiding low-temperature re-equilibration. Although the mechanism of formation of porphyroclastic texture is still in dispute, we interpret this higher temperature as a peak metamorphic temperature of the Napier UHT metamorphism. On the other hand, the lower temperatures (650–700°C) as obtained by the compositions of granular and neoblastic pyroxenes could represent the temperature equilibrated during the retrograde stage after the peak metamorphism, at which time redistribution of elements in pyroxenes, probably accompanied by the formation of exsolution lamellae, may have been diminished. It is, therefore, possible that the lower temperature means that a lower limit was imprinted in pyroxene compositions. The formation of neoblastic pyroxenes may have been attributed to a kind of deformation process during the retrograde stage; *i.e.*, if porphyroclastic pyroxenes locally evaded such a process and preserved the compositions of the peak metamorphic temperature, then neoblastic pyroxenes would have been formed along or around the porphyroclastic pyroxenes during that process. Inasmuch as exsolution lamellae develop characteristically in neoblastic pyroxenes, this process may have also been related to the low-temperature

redistribution of elements.

Previous thermometric approaches using chemical compositions of constituent minerals for the Napier Complex include Sandiford and Powell (1986, 1988), Harley (1987), Harley and Motoyoshi (2000) and Hokada (2001). Of these, Sandiford and Powell (1986, 1988) and Harley (1987) have deduced metamorphic temperatures of up to 1020°C for the Napier UHT metamorphism based on the study of inverted pigeonite in meta-ironstone, and Harley (1987) estimated 890–990°C based on the compositions of porphyroclastic pyroxenes in ultramafic granulites. Harley and Motoyoshi (2000) used the alumina content of porphyroblastic orthopyroxene from the sapphirine+orthopyroxene+quartz granulite to deduce a temperature in excess of 1120°C. Hokada (2001) observed feldspar with perthite or antiperthite texture, calculated the compositions of one-phase feldspar that had been once stable at peak temperature, and then estimated the temperature to have been about 1100°C by using the feldspar thermometer. The peak temperatures estimated in the present study are generally consistent with these previous studies, indicating again evidence for UHT (>1000°C) metamorphism in the Napier Complex.

Although the approach of the present study is similar to Harley (1987), the present results (up to 1130°C) indicate higher temperature than those (890–990°C) of Harley (1987). The porphyroclastic pyroxenes described by Harley (1987) occur on East Tonagh Island, about 50 km southwest of the Mt. Riiser-Larsen area (Fig. 1). Also, Harley (1987) described inverted pigeonite from meta-ironstone in the same area, and estimated about 980°C, which is also lower than the temperature (about 1100°C) estimated from compositions of inverted pigeonite from the Mt. Riiser-Larsen area (Ishizuka *et al.*, in prep.). A recent detailed study of Tonagh Island, several km northwest of East Tonagh Island (Osanai *et al.*, 1999), showed rare occurrences of osumilite and sapphirine+quartz that are diagnostic of UHT metamorphism. It follows that the peak metamorphic temperature may be different between East Tonagh Island and the Mt. Riiser-Larsen area, although Hokada (2001), who estimated temperatures by mineral compositions of mesoperthitic alkali feldspar from Tonagh Island and the Mt. Riiser-Larsen area, indicated no significant difference in peak metamorphic temperature between these two areas. Further comparative study is needed to elucidate the regional difference or similarity in peak metamorphic conditions of the Napier UHT metamorphism.

Acknowledgments

We would like to thank Drs. M. Ishikawa and T. Hokada for their co-operation in the field work and helpful discussion during this study.

References

Harley, S.L. (1987): A pyroxene-bearing meta-ironstone and other pyroxene-granulites from Tonagh Island, Enderby Land, Antarctica: further evidence for very high temperature (>980°C) Archaean regional metamorphism in the Napier Complex. J. Metamorph. Geol., **5**, 341–356.

Harley, S.L. (1998): On the occurrence and characterization of ultrahigh-temperature crustal metamorphism. What Drives Metamorphism and Metamorphic Reactions ?, ed. by P.J. Treloar and P. O'Brien, 75–101.

Harley, S.L and Motoyoshi, Y (2000). Al zoning in orthopyroxene in a sapphirine quartzite: evidence for >1120°C UHT metamorphism in the Napier Complex, Antarctica, and implications for the entropy of sapphirine Contrib. Mineral. Petrol., **138**, 293-307

Hokada, T (2001): Feldspar thermometry in ultrahigh-temperature metamorphic rocks: evidence of crustal metamorphism attaining ~1100°C in the Archaean Napier Complex, East Antarctica Am. Mineral, **86**, 932-938.

Ishikawa, M., Hokada, T., Ishizuka, H, Miura, H, Suzuki, S., Takada, M. and D.P Zwartz (2000) Antarctic Geological Map Series, Sheet 37, Mount Riiser-Larsen, with explanatory text (23 p) Tokyo. National Institute of Polar Research.

Ishizuka, H, Ishikawa, M., Hokada, T and Suzuki, S. (1998): Geology of the Mt Riiser-Larsen area of the Napier Complex, Enderby Land, East Antarctica Polar Geosci, **11**, 154-171

Lindsley, D.H (1983) Pyroxene thermometry Am Mineral., **68**, 477-493

Osanai, Y, Toyoshima, T., Owada, M, Tsunogae, T, Hokada, T and Crowe, A W. (1999): Geology of ultrahigh-temperature metamorphic rocks from Tonagh Island in the Napier Complex, East Antarctica. Polar Geosci, **12**, 1-28.

Spear, S F. (1993). Metamorphic Phase Equilibria and Pressure-Temperature-Time Paths Washington, D C, Mineralogical Society of America, 799 p

Sandiford, M and Powell, R (1986): Pyroxene exsolution in granulites from Fyfe Hills, Enderby Land, Antarctica. Evidence for 1000°C metamorphic temperatures in Archaean continental crust Am Mineral, **71**, 946-954.

Sandiford, M and Powell, R. (1988) Pyroxene exsolution in granulites from Fyfe Hills, Enderby Land, Antarctica Evidence for 1000°C metamorphic temperatures in Archaean continental crust—Reply Am Mineral, **73**, 434-438

Suzuki, S, Hokada, T, Ishikawa, M and Ishizuka, H (1999): Geochemical study of granulites from Mt Riiser-Larsen, Enderby Land, East Antarctica. Implication for protoliths of the Archaean Napier Complex Polar Geosci., **12**, 101-125.

Wells, P R A (1977). Pyroxene thermometry in simple and complex systems Contrib. Mineral. Petrol., **62**, 129-139

Wood, B.J. and Banno, S (1973) Garnet-orthopyroxene and orthopyroxene-clinopyroxene relationships in simple and complex systems. Contrib Mineral Petrol., **42**, 109-124

(Received April 8, 2002, Revised manuscript accepted May 24, 2002)